AD-A147 830 ELECTRICAL RESISTIVITY IN LOW RESISTIVITY AMORPHOUS ALLOYS(U) ARMY ARMAMENT RESEARCH AND DEVELOPMENT CENTER WATERVLIET NY L. L V MEISEL ET AL. OCT 84 1/1

UNCLASSIFIED ARLCB-TR-84030 SBI-AD-E440 258 F/G 20/3 NL

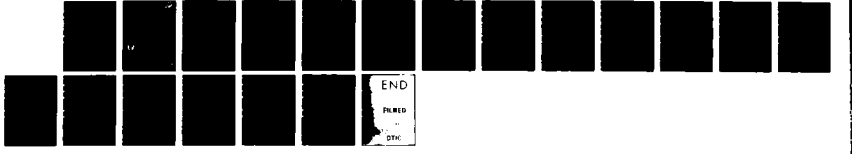

END

FILMED

DTIC

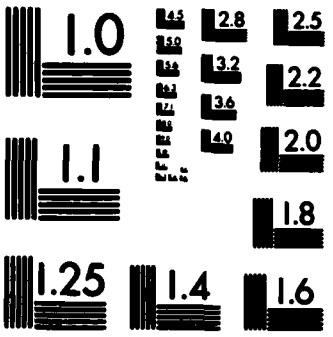

MICROCOPY RESOLUTION TEST CHART
NATIONAL BUREAU OF STANDARDS-1963-A

TECHNICAL REPORT ARLCB-TR-84030

ELECTRICAL RESISTIVITY IN LOW RESISTIVITY AMORPHOUS ALLOYS

L. V. MEISEL
P. J. COTE

OCTOBER 1984

US ARMY ARMAMENT RESEARCH AND DEVELOPMENT CENTER
LARGE CALIBER WEAPON SYSTEMS LABORATORY
BENÉT WEAPONS LABORATORY
WATERVLIET N.Y. 12189

DISCLAIMER

The findings in this report are not to be construed as an official Department of the Army position unless so designated by other authorized documents.

The use of trade name(s) and/or manufacture(s) does not constitute an official indorsement or approval.

DISPOSITION

Destroy this report when it is no longer needed. Do not return it to the originator.

SECURITY CLASSIFICATION OF THIS PAGE (When Data Entered)

REPORT DOCUMENTATION PAGE		READ INSTRUCTIONS BEFORE COMPLETING FORM
1. REPORT NUMBER ARLCB-TR-84030	2. GOVT ACCESSION NO. AD-A147830	3. RECIPIENT'S CATALOG NUMBER
4. TITLE (and Subtitle) ELECTRICAL RESISTIVITY IN LOW RESISTIVITY AMORPHOUS ALLOYS		5. TYPE OF REPORT & PERIOD COVERED Final 6. PERFORMING ORG. REPORT NUMBER
7. AUTHOR(s) L. V. Meisel and P. J. Cote		8. CONTRACT OR GRANT NUMBER(s)
9. PERFORMING ORGANIZATION NAME AND ADDRESS US Army Armament Research & Development Center Benet Weapons Laboratory, SMCAR-LCB-TL Watervliet, NY 12189		10. PROGRAM ELEMENT, PROJECT, TASK AREA & WORK UNIT NUMBERS AMCMS No.6111.02.H600.011 Pron No.1A325B541A1A
11. CONTROLLING OFFICE NAME AND ADDRESS US Army Armament Research & Development Center Large Caliber Weapon Systems Laboratory Dover, NJ 07801		12. REPORT DATE September 1984 13. NUMBER OF PAGES 11
14. MONITORING AGENCY NAME & ADDRESS(if different from Controlling Office)		15. SECURITY CLASS. (of this report) Unclassified 15a. DECLASSIFICATION/DOWNGRADING SCHEDULE

16. DISTRIBUTION STATEMENT (of this Report)

Approved for Public Release, Distribution Unlimited

17. DISTRIBUTION STATEMENT (of the abstract entered in Block 20, if different from Report)

18. SUPPLEMENTARY NOTES

Presented at the Fifth International Conference on Liquid & Amorphous Metals, Los Angeles, California, 15-19 August 1983

19. KEY WORDS (Continue on reverse side if necessary and identify by block number)

Amorphous Alloys
Electron Transport
Diffraction Model
Saturation

20. ABSTRACT (Continue on reverse side if necessary and identify by block number)

The temperature dependence of the electrical resistivity in low resistivity ($\rho < 100\ \mu\Omega$cm) amorphous alloys is analyzed in the framework of the diffraction model. The standard diffraction model yields results in qualitative agreement with the available data. However, a quantitative agreement with the data is observed if phonon ineffectiveness effects are included by means of the Pippard-Ziman constraint. A variety of results are presented for ranges of $2k_F/k_p$ and electron mean free paths.

DD FORM 1 JAN 73 1473 EDITION OF 1 NOV 65 IS OBSOLETE

UNCLASSIFIED

SECURITY CLASSIFICATION OF THIS PAGE (When Data Entered)

BLANK PAGE

TABLE OF CONTENTS

LIST OF ILLUSTRATIONS

INTRODUCTION

The diffraction model (ref 1) provides the basis for quantitative studies of electrical transport in liquid and amorphous metals. Surprisingly good agreement with experimental data has been obtained. However, significant discrepancies between diffraction model predictions and the data are well known in high resistivity ($\rho > 100$ $\mu\Omega$cm) amorphous metals. Such discrepancies are called saturation effects (ref 2).

Recently, detailed experimental electrical transport studies of low resistivity amorphous alloys have been reported (ref 3). The present authors reported diffraction model studies (ref 4) of these alloys employing an effective t-matrix adjusted to satisfy the Friedel sum rule and to yield the observed magnitude of ρ. The surprising result of the theoretical analysis was that although qualitative agreement with the experimental results was obtained with the standard diffraction model, substantially improved quantitative agreement was obtained when saturation effects were incorporated into the model in a manner consistent with that employed to treat saturation effects in high resistivity metals (ref 5). That is, improved agreement with experiment was obtained when the Pippard-Ziman constraint (ref 6) on the electron-phonon interaction was included. (It had been shown previously that the Pippard-Ziman constraint can also provide a basis for understanding the electronic contribution to the ultrasonic attenuation (ref 6) at small qA, and the degradation of T_c in disordered superconductors (ref 7).)

References are listed at the end of this report.

The implications of the diffraction model incorporating phonon ineffectiveness through the Pippard-Ziman constraint for low resistivity alloys are explored in more detail in this report. A broader class of t-matrices as well as larger ranges of Λ and $2k_F/k_p$ than in Reference 4 are treated. We work in the context of the substitutional model (ref 8), which assumes the equality of all partial structure factors, but allows for different t-matrices for different species; thus, a better basis for interpretation of concentration dependent features of the T dependence of ρ than can be obtained in an effective potential treatment (ref 4) is established. We also restrict our analysis to binary alloys. The results specific to amorphous magnesium zinc (a-MgZn) alloys, for which $q_D\Lambda$ ranges between about 12 and 15 and $2k_F/k_p \approx 1.1$ are reported in Reference 9.

THEORETICAL MODELS

The diffraction model (ref 1) (Ziman-Faber theory) result for the electrical resistivity is

$$\rho = \frac{12\pi\Omega_o}{e^2hV_F^2} \int_0^1 d[\frac{K}{2k_F}][\frac{K}{2k_F}]^3|U(K)|^2 \qquad (1)$$

where Ω_o is the atomic volume, V_F is the Fermi velocity, k_F is the Fermi wavevector, K is the scattering vector, h is Planck's constant divided by 2π, e is the electron charge, and in the "substitutional model," assuming a Debye phonon spectrum, and a binary alloy

$$|U(K)^2| = c_1c_2|t_1(K) - t_2(K)|^2 I^\rho(K) + |c_1t_1(K) + c_2t_2(K)|^2 S^\rho(K) \qquad (2)$$

where c_i and $t_i(K)$ are the concentration and t-matrix for the i^{th} component,

$$S^{\rho}(K) = e^{-2W(K)}a(K) + \alpha \frac{\theta}{T}\left(\frac{K}{2k_F}\right)^2 \int_0^1 d\left(\frac{q}{q_D}\right)\left(\frac{q}{q_D}\right)^2 n(x)(n(x)+1)F(q\Lambda)\int \frac{d\Omega q}{4\pi} a(\vec{K}+\vec{q}) \quad (3)$$

and

$$I^{\rho}(K) = e^{-2W(K)} + \alpha \frac{\theta}{T}\left(\frac{K}{2k_F}\right)^2 \int_0^1 d\left(\frac{q}{q_D}\right)\left(\frac{q}{q_D}\right)^2 n(x)[n(x)+1]F(q\Lambda) \quad (4)$$

in Sham-Ziman approximation. Here $e^{-2W(K)}$ is the Debye-Waller factor, $x = (\theta/T)(q/q_D)$, q_D the Debye wave number, θ the Debye temperature, T the temperature, $n(x) = (e^x-1)^{-1}$, $\alpha = 3(2\hbar k_F)^2/Mk_B\theta$, M is the averaged ionic mass, k_B is Boltzmann's constant. F(qA) is referred to as the Pippard function and is given by

$$F(y) = \frac{2}{\pi}\left[\frac{y \tan^{-1} y}{y-\tan^{-1} y} - \frac{3}{y}\right] \quad (5)$$

We refer to $S^{\rho}(K)$ as the resistivity static structure factor. $I^{\rho}(K)$ is the resistivity static structure factor for a perfectly random array. $S^{\rho}(K)$ and $I^{\rho}(K)$ determine the temperature dependences of electrical transport quantities.

The geometric structure factors (assumed identical in the substitutional model) are given by

$$a(K) = a_{11}(K) = a_{22}(K) = a_{12}(K) = \frac{1}{N}\sum_{m,n} \exp[i\vec{K}\cdot(\vec{m}-\vec{n})] \quad (6)$$

where m and n run over averaged ionic positions. The scattering matrix elements (which incorporate single site multiple scattering) are given by

$$t_j(K) = \frac{2\pi\hbar^3}{m(2mE_F)^{1/2}\Omega_0}\sum(2\ell+1)\sin\eta_\ell^j(E_F)e^{i\eta_\ell^j(E_F)}P_\ell(\cos\theta) \quad (7)$$

where $n_\ell{}^j(E_F)$ is the scattering phase shift for angular momentum quantum number ℓ evaluated at the Fermi energy E_F for the j^{th} constituent, m is the electron mass, $P_\ell(x)$ is the ℓ^{th} Legendre polynomial and $\cos\theta = 1 - 2(K/2k_F)^2$. These equations are a generalization of those usually employed in studies of transport in liquid metals (ref 10) and will be discussed in more detail elsewhere.

We also give results based on the effective potential model. In this model, $t_1(K) \cong t_2(K) \cong t_E(K)$ and

$$|U_E(K)|^2 = S_E\rho(K)|t_E(K)|^2 \tag{8}$$

where $S_E{}^\rho(K)$ is defined analogously to $S^\rho(K)$ in Eq. (3) with the effective geometrical structure factor

$$a_E(K) = \sum_{ij} c_i c_j a_{ij}(K) \tag{9}$$

RESULTS

Results are given for an effective potential and for model t-matrices in a binary substitutional model. Percus-Yevick hard sphere structure factors (ref 11) (with packing fraction 0.525) are used to approximate a(K) and $a_E(K)$; the hard sphere diameters are varied to adjust $2k_F/k_p$ where k_p is the position of the principal structure factor peak.

The effective potential has phase shifts $\eta_\ell(E_F)$ given by 0.354, 0.294, -0.057, and 0.002 for $\ell = 0,1,2,3$, respectively, which yield approximate cancellation for $K \approx 1.6\ k_F$ and lead to ρ vs. T curves similar to those obtained in Reference 4 for Born approximation pseudopotentials in the large $q_D\Lambda$ limit. However, this effective potential heavily weighs backscattering and so is quite different in form from pseudopotentials. (These $\eta_\ell(E_F)$ were

computed for Zn with $X_\alpha = 0.85$.)

The t-matrices employed in the substitutional model calculations were computed using Herman and Skillman (ref 12) neutral atom wavefunctions for a-Mg_7Zn_3. The values of $\eta[\ell](E_F)$ are: -0.175, 0.085, 0.034, and 0.001 for Mg and 0.354, 0.294, -0.057, and 0.002 for Zn (as in the effective potential) for $\ell = 0$ to 3, respectively. (The phase shifts are quite sensitive to exchange. X_α was taken as 0.75 and 0.85 in Mg and Zn, respectively.) Very similar results (not discussed here) have been obtained for other t-matrices constructed to represent column I and column II metals in the substitutional model.

DISCUSSION OF RESULTS

The Temperature Coefficient of Resistivity (TCR)

Figure 1 shows graphs of tcr, the normalized TCR, where

$$tcr \equiv (\theta/\alpha)\cdot TCR = (\theta/\alpha\rho)d\rho/dT|\theta$$

versus $2k_F/k_p$ for the two model potentials.

All the results were obtained with E_F fixed and $q_D = k_F$ which would not apply in an alloy series with varying electron-to-atom ratios. The curves were computed for $\alpha = 0.114$, but are very good approximations for reasonable values of α. One sees a shift of the region of negative TCR to larger values of $2k_F/k_p$ with respect to the results of the simple analysis based on the temperature dependence of the resistivity static structure factor by Meisel and Cote (ref 13). Futhermore, analysis of data in a-MgZn alloys indicates that 50 $\mu\Omega$cm corresponds to $q_D\Lambda$ near 12 which produces dramatic changes in the TCR from the predictions of standard ($q_D\Lambda = \infty$) Ziman-Faber theory.

Comparison of Figures 1(a) and 1(b) illustrates non-structural effects (i.e., effects produced by different scattering matrices) that might occur. One can also infer that (especially in cases for which $q_D\Lambda < 15$) the averaging required in treating real binary alloys - whose partial structure factor peaks might be separated by $k_p/10$ - would not yield qualitatively new effects; for example, about the same range of $2k_F/k_p$ would yield negative TCR.

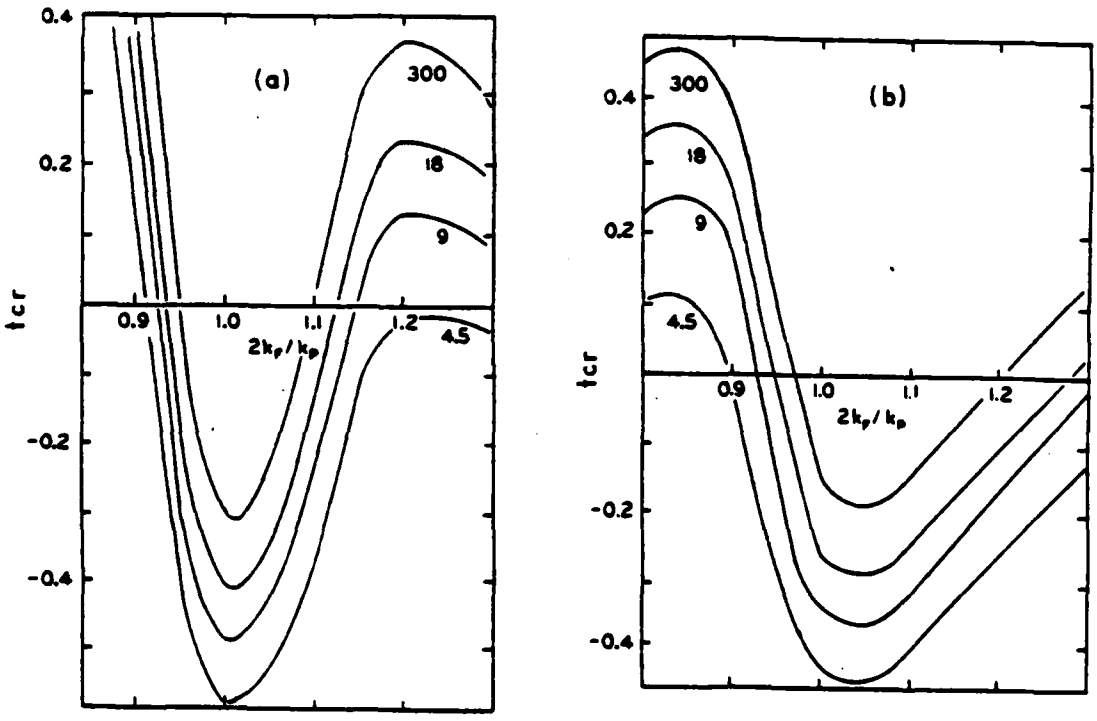

Figure 1. Normalized TCR vs. $2k_F/k_p$ for various $q_D\Lambda$. (a) For the effective potential. (b) For the substitutional model. $q_D\Lambda$ is indicated for each curve.

The Temperature Dependence of the Electrical Resistivity

Figure 2 shows results of calculations at various values of $2k_F/k_p$ and $q_D\Lambda$ for the substitutional model potential and also at $2k_F/k_p = 1.1$ for $q_D\Lambda = 8$ for the effective potential case. (Results at $2k_F/k_p = 1.11$ for the substitutional model applied to a-MgZn are shown in Reference 9. The graphs show the normalized relative change in the resistivity,

$$r \equiv (\rho(T) - \rho(\theta)/(\alpha\rho(\theta))$$

plotted against normalized temperature. (Most results were computed for $\alpha = 0.168$ but hold for reasonable α.)

The results show that deviations from standard diffraction model predictions can be explained by incorporating phonon ineffectiveness effects into the theory.

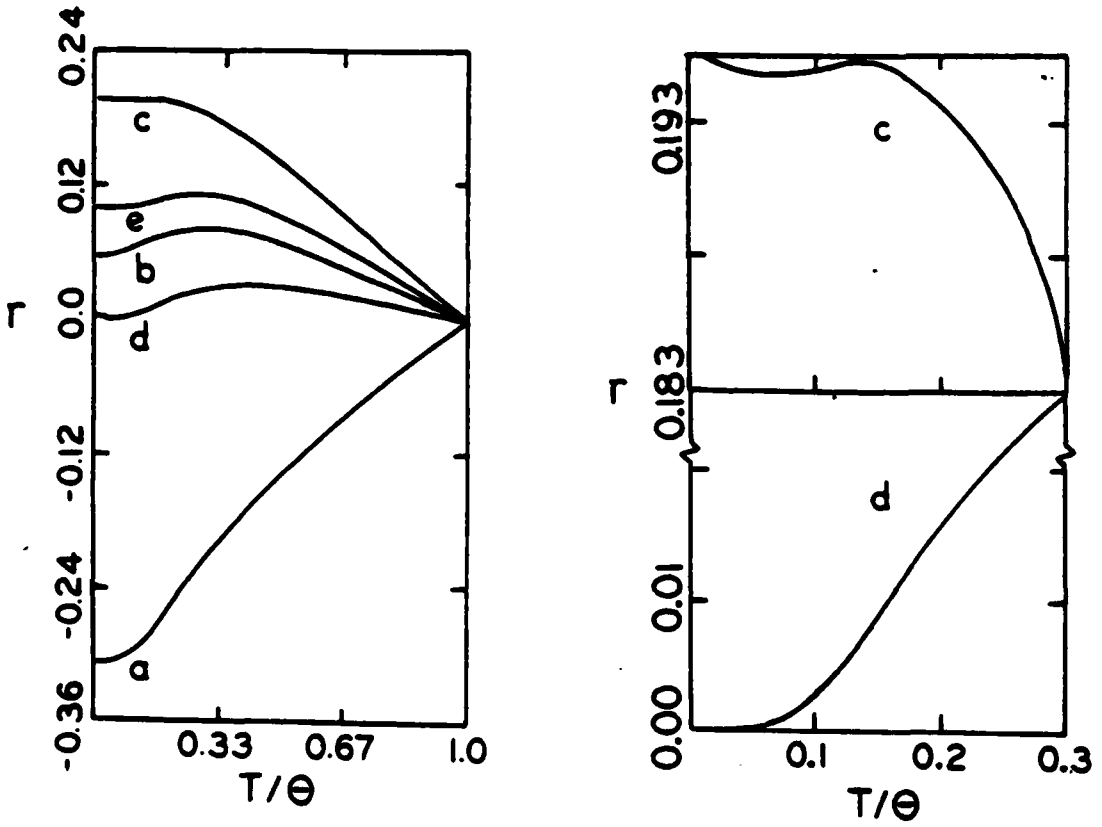

Figure 2. Normalized relative change in the resistivity vs. normalized temperature. Curves a-d are for the substitutional model. Curve e is for the effective potential. Details of curves c and d are shown below.

Curve	a	b	c	d	e
2kF/kp	0.9	1.0	1.0	1.2	1.1
$q_D\Lambda$	18	300	12	12	8

REFERENCES

1. R. Evans, B. L. Gyorffy, N. Szabo, and J. M. Ziman, "On the Resistivity of Liquid Transition Metals," in: The Properties of Liquid Metals, (S. Takeuchi, ed.), John Wiley and Sons, New York, 1973; T. E. Faber, Introduction to the Theory of Liquid Metals, Cambridge U. Press, Cambridge, 1972, Ch V and VI; Baym, Phys. Rev. A135, 1964, p. 1691; J. M. Ziman, Phil. Mag. 6, 1961, p. 1013; P. J. Cote and L. V. Meisel, "Electrical Transport in Amorphous Metals," in: Topics in Applied Physics, Vol. 46, (H.-J. Guntherodt and H. Beck, eds.).
2. See, for example, J. H. Mooij, Phys. Status Solidi A17, 1973, p. 521 or Cote and Meisel in Reference 1.
3. Particularly, T. Matsuda and U. Mizutani, J. Phys. F12, 1982, p. 1877 and U. Mizutani and K. Yoshina, J. Phys. F, (in press).
4. L. V. Meisel and P. J. Cote, Phys. Rev. B27, 1983, p. 4617.
5. P. J. Cote and L. V. Meisel, Phys. Rev. Lett. 40, 1978, p. 1586 and in Reference 1.
6. A. B. Pippard, Philos. Mag. 46, 1955, p. 1140; J. M. Ziman, Electrons and Phonons, Clarendon Press, Oxford.
7. N. Morton, B. W. James, G. H. Wostenholm, Cyrogenics 18, 1978, p. 131 and L. V. Meisel and P. J. Cote, Phys. Rev. B19, 1979, p. 4514.
8. T. E. Faber and J. M. Ziman, Philos. Mag. 11, 1965, p. 153.
9. P. J. Cote and L. V. Meisel, "Application of the Diffraction Model to Amorphous Magnesium Zinc Alloys," U.S. ARDC Technical Report ARLCB-TR-84031, Benet Weapons Laboratory, Watervliet, NY, October 1984.

10. L. V. Meisel and P. J. Cote, Phys. Rev. B16, 1977, p. 2978; P. J. Cote and L. V. Meisel, Phys. Rev. Lett. 39, 1977, p. 102; see also K. Frobose and J. Jackle, J. Phys. F7, 1977, p. 2331; F. J. Ohkawa, Inst. Sol. State Physics A842, 1977; and Reference 1.

11. J. K. Percus and G. J. Yevick, Phys. Rev. 110, 1958, p. 1 and J. L. Lebowitz, Phys. Rev. 133, 1964, p. A895.

12. F. C. Herman and S. Skillman, Atomic Structure Calculations, Prentice Hall, Englewood Cliffs, NJ, 1963.

13. L. V. Meisel and P. J. Cote, Phys. Rev. B17, 1978, p. 4652.

TECHNICAL REPORT INTERNAL DISTRIBUTION LIST

	NO. OF COPIES
CHIEF, DEVELOPMENT ENGINEERING BRANCH	
ATTN: SMCAR-LCB-D	1
-DA	1
-DP	1
-DR	1
-DS (SYSTEMS)	1
-DS (ICAS GROUP)	1
-DC	1
CHIEF, ENGINEERING SUPPORT BRANCH	
ATTN: SMCAR-LCB-S	1
-SE	1
CHIEF, RESEARCH BRANCH	
ATTN: SMCAR-LCB-R	2
-R (ELLEN FOGARTY)	1
-RA	1
-RM	2
-RP	1
-RT	1
TECHNICAL LIBRARY	5
ATTN: SMCAR-LCB-TL	
TECHNICAL PUBLICATIONS & EDITING UNIT	2
ATTN: SMCAR-LCB-TL	
DIRECTOR, OPERATIONS DIRECTORATE	1
DIRECTOR, PROCUREMENT DIRECTORATE	1
DIRECTOR, PRODUCT ASSURANCE DIRECTORATE	1

NOTE: PLEASE NOTIFY DIRECTOR, BENET WEAPONS LABORATORY, ATTN: SMCAR-LCB-TL, OF ANY ADDRESS CHANGES.

TECHNICAL REPORT EXTERNAL DISTRIBUTION LIST

	NO. OF COPIES
ASST SEC OF THE ARMY RESEARCH & DEVELOPMENT ATTN: DEP FOR SCI & TECH THE PENTAGON WASHINGTON, D.C. 20315	1
COMMANDER DEFENSE TECHNICAL INFO CENTER ATTN: DTIC-DDA CAMERON STATION ALEXANDRIA, VA 22314	12
COMMANDER US ARMY MAT DEV & READ COMD ATTN: DRCDE-SG 5001 EISENHOWER AVE ALEXANDRIA, VA 22333	1
COMMANDER ARMAMENT RES & DEV CTR US ARMY AMCCOM	
ATTN: SMCAR-LC	1
SMCAR-LCE	1
SMCAR-LCM (BLDG 321)	1
SMCAR-LCS	1
SMCAR-LCU	1
SMCAR-LCW	1
SMCAR-SCM-O (PLASTICS TECH EVAL CTR, BLDG. 351N)	1
SMCAR-TSS (STINFO) DOVER, NJ 07801	2
DIRECTOR BALLISTICS RESEARCH LABORATORY ATTN: AMXBR-TSB-S (STINFO) ABERDEEN PROVING GROUND, MD 21005	1
MATERIEL SYSTEMS ANALYSIS ACTV ATTN: DRXSY-MP ABERDEEN PROVING GROUND, MD 21005	1
COMMANDER US ARMY AMCCOM ATTN: SMCAR-ESP-L ROCK ISLAND, IL 61299	1
COMMANDER ROCK ISLAND ARSENAL ATTN: SMCRI-ENM (MAT SCI DIV) ROCK ISLAND, IL 61299	1
DIRECTOR US ARMY INDUSTRIAL BASE ENG ACTV ATTN: DRXIB-M ROCK ISLAND, IL 61299	1
COMMANDER US ARMY TANK-AUTMV R&D COMD ATTN: TECH LIB - DRSTA-TSL WARREN, MI 48090	1
COMMANDER US ARMY TANK-AUTMV COMD ATTN: DRSTA-RC WARREN, MI 48090	1
COMMANDER US MILITARY ACADEMY ATTN: CHMN, MECH ENGR DEPT WEST POINT, NY 10996	1
US ARMY MISSILE COMD REDSTONE SCIENTIFIC INFO CTR ATTN: DOCUMENTS SECT, BLDG. 4484 REDSTONE ARSENAL, AL 35898	2
COMMANDER US ARMY FGN SCIENCE & TECH CTR ATTN: DRXST-SD 220 7TH STREET, N.E. CHARLOTTESVILLE, VA 22901	1

NOTE: PLEASE NOTIFY COMMANDER, ARMAMENT RESEARCH AND DEVELOPMENT CENTER, US ARMY AMCCOM, ATTN: BENET WEAPONS LABORATORY, SMCAR-LCB-TL, WATERVLIET, NY 12189, OF ANY ADDRESS CHANGES.

TECHNICAL REPORT EXTERNAL DISTRIBUTION LIST (CONT'D)

	NO. OF COPIES
COMMANDER US ARMY MATERIALS & MECHANICS RESEARCH CENTER ATTN: TECH LIB - DRXMR-PL WATERTOWN, MA 01272	2
COMMANDER US ARMY RESEARCH OFFICE ATTN: CHIEF, IPO P.O. BOX 12211 RESEARCH TRIANGLE PARK, NC 27709	1
COMMANDER US ARMY HARRY DIAMOND LAB ATTN: TECH LIB 2800 POWDER MILL ROAD ADELPHIA, MD 20783	1
COMMANDER NAVAL SURFACE WEAPONS CTR ATTN: TECHNICAL LIBRARY CODE X212 DAHLGREN, VA 22448	1
DIRECTOR US NAVAL RESEARCH LAB ATTN: DIR, MECH DIV CODE 26-27, (DOC LIB) WASHINGTON, D.C. 20375	1 1
COMMANDER AIR FORCE ARMAMENT LABORATORY ATTN: AFATL/DLJ AFATL/DLJG EGLIN AFB, FL 32542	1 1
METALS & CERAMICS INFO CTR BATTELLE COLUMBUS LAB 505 KING AVENUE COLUMBUS, OH 43201	1

NOTE: PLEASE NOTIFY COMMANDER, ARMAMENT RESEARCH AND DEVELOPMENT CENTER, US ARMY AMCCOM, ATTN: BENET WEAPONS LABORATORY, SMCAR-LCB-TL, WATERVLIET, NY 12189, OF ANY ADDRESS CHANGES.

END

FILMED

12-84

DTIC